Optical Fiber Technology 72 (2022) 102980

Contents lists available at ScienceDirect

Optical Fiber Technology

journal homepage: www.elsevier.com/locate/yofte

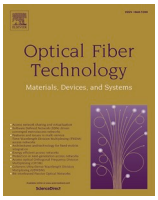

Temperature effects on the emission of polymer optical fibers doped with Lumogen dyes

Jon Grandes [a,*], María Asunción Illarramendi [a], Eneko Arrospide [b], Iñaki Bikandi [c], Ibon Aramburu [a], Nekane Guarrotxena [d], Olga García [d], Joseba Zubia [c]

[a] Department of Applied Physics, University of the Basque Country (UPV/EHU), Engineering School of Bilbao (EIB), Plaza Ingeniero Torres Quevedo 1, E-48013 Bilbao, Spain
[b] Department of Applied Mathematics, University of the Basque Country (UPV/EHU), Engineering School of Bilbao (EIB), Spain
[c] Department of Communications Engineering, University of the Basque Country (UPV/EHU), School of Bilbao (EIB), Spain
[d] Instituto de Ciencia y Tecnología de Polímeros, Consejo Superior de Investigaciones Científicas (ICTP-CSIC), Juan de la Cierva 3, E-28006 Madrid, Spain

ARTICLE INFO

Keywords:
Polymer optical fiber
Temperature effects
Thermal damage
Luminescent materials
Luminescent solar concentrators
Green energy

ABSTRACT

In this paper, we report the temperature effects on the luminescence of polymer optical fibers doped with Lumogen dyes (red and orange). Specifically, we have analyzed the intensity and the average wavelength of the spectra emitted by both fibers when they are heated from 30 °C to 90 °C. An almost full self–recovery of the signal in the fiber doped with Lumogen red has been observed when the fiber is subjected to thermal cycles with oscillating temperature variations between 30 °C and 90 °C. The emitted spectra are red/blue shifted when the fiber sample is heated/cooled with a final temperature sensitivity around 0.07 nm/°C when a stationary situation is reached.

1. Introduction

Polymer optical fibers (POFs) have historically occupied a niche in the optical fiber world thanks to their robustness, large core diameters, high numerical apertures, and low cost [1]. Particularly, in the last years they have been widely used both for short-haul communications links, where distances to cover are generally less than 1 km and for a whole range of different sensing applications. When the POFs are doped with functional materials, such as organic dyes, ions of rare earths, quantum dots or noble metal nanoparticles, they can offer a wide range of applications in the fields of lasers, optical amplifiers, illuminators, switches, sensors or solar concentrators [2].

Doped polymer optical fibers can be operated as luminescent solar concentrators (LSCs). The absorbed sunlight through their lateral surface is re-emitted as fluorescence light at greater wavelengths and this is propagated by total internal reflection to the fiber ends, where the photovoltaic (PV) cells are placed. The concept of LSCs was introduced in the 1970s with the objective of reducing the cost of solar cells [3]. Due to the important development of new materials and of the utmost urgency of sustainable global development, research on LSCs has recently regained momentum. In this process of research, one of the characteristics studied is the geometric form of the concentrator, such as cylindrical LSCs. The studies about LSCs of cylindrical shape have been carried out with optical fibers in most cases (e.g., doped POFs of different geometries, melt-spun POFs, or electrospun nanofibers) [4–9]. Unlike traditional planar rectangular LSCs, doped POFs have a better coupling between their ends and the PV cells and, they can easily be connected to other nondoped POFs, to allow spatial separation between the light collection and detection systems, if necessary. All these properties, combined with commonly available materials and ease of processing, make fluorescent fiber solar concentrators an attractive option in the area of LSCs [10–12]. For example, they can be employed in applications as building integrated photovoltaics (BIPVs) in cities, or as powerful and highly adaptive photonic platforms, such as displays, chemical reactors, dark-field imaging or several sensing applications [12].

As LSCs become more viable for real applications, it is necessary to get to know precisely their performance under realistic external conditions. For example, thermal damage is produced in LSCs due to the high temperatures reached under solar radiation, in sunny days on the Earth or in the Space [13]. It is well known that the heat deteriorates substantially the performance of the solar cells. Specifically, the efficiency

* Corresponding author.
E-mail address: jon.grandes@ehu.eus (J. Grandes).

https://doi.org/10.1016/j.yofte.2022.102980
Received 10 February 2022; Received in revised form 13 June 2022; Accepted 7 July 2022
Available online 18 July 2022

of a crystalline silicon solar cell decreases 0.5 % for every 1 °C above 25 °C [14]. The solar cell temperature can reach values well above 50 °C, which implies significant performance loss of the solar cell. The operating temperatures of the PV cells when they are attached to LSCs are cooler (up to 10 °C) comparing to the temperatures of cells facing direct solar exposure [15]. This effect is due to both the avoidance of infrared sunlight impinging on the attached cells and the good spectral matching between the emission of LSCs and the response of PV cells. Taking into account all these considerations and that LSCs are exposed to direct radiation from the sun, studies about the thermal performance of LSCs can be very useful in this application area.

The photoinduced thermal degradation in dye-doped polymer matrices mainly brings about a chemical process in which the functional bonds of dye molecules are changed and broken. As a result, the dye molecules may cease to produce fluorescence or produce different fluorescence. The photoinduced degradation of materials from which LSCs are made, has been studied by exposing samples to lasers or UV radiation [16–18]. However little has been investigated about thermal effects on the properties of LSC devices [19,20]. The study of the temperature effects on the efficiency of LSCs can help to improve the stability of these devices, for example, if they are used in space solar power systems [13]. An efficient heat dissipation can minimize the thermal degradation of the performance of LSCs and it can become an essential matter when LSCs are in high temperature environments. Taking into account that the cylindrical geometry of fibers contributes to dissipate the heat generated, an investigation of the thermal effects in LSCs based in doped polymer optical fibers can provide valuable information in order to develop strategic geometries and dispositions of LCSs.

In this work, we report the temperature dependence of the emission spectra in the range 30–90 °C for two different fluorescent fiber solar concentrators. Although it is difficult for LSCs to reach this temperature on the Earth surface, they can be exposed to higher temperatures than 90 °C if they are used in space satellites [13]. The luminescent fibers are POFs doped with two different active dye derivatives from perylene, namely Lumogen red (LR) and Lumogen orange (LO). Although PMMA has not a good heat resistance, it is an excellent candidate to be used as polymeric matrix due to its good chemical stability and biocompatibility, high transparency over a wide spectral range, high refraction index and easy processability. On the other hand, Lumogen dyes have been extensively and successfully employed in LSCs, and they are still being studied nowadays [21–23]. We analyze the influence of temperature on the emitted fluorescence characteristics, such as the intensity and the average wavelength, by subjecting doped POFs to several temperature dependent measurements, including thermal cycles.

2. Experimental

Fig. 1 shows the experimental set-up used to study the temperature effects on the fluorescence spectra emitted from doped fibers. The fibers were heated up by means of a climate chamber CTS C–70/200 model, (CTS GmbH, Germany). The furnace had two openings that allowed the introduction of a light source to illuminate the fibers and all the necessary wiring for detection. In addition to the fiber sample to be analyzed, a thermocouple (type-K thermocouple with 0.5 °C resolution) was introduced into the furnace next to the fiber so that the temperature of the sample could be accurately measured. The analyzed sample was connected to a silica multimode optical fiber to transmit the emitted light up to a fiber-optic spectrometer (Avantes model AvaSpec-Mini, with an optical resolution of 1.4 nm of full width at half maximum) for the measurement of the emission spectra. The thermocouple was connected to an USB device, which allowed the collecting of the temperature data. The light source used to illuminate the fibers was a 60 W incandescent bulb designed to withstand temperatures up to 300 °C. The end of the fiber sample that is not connected to the detector was fixed to a metallic grid placed inside the furnace and it was covered so that the light source illuminates the fiber sample along its lateral surface only. The small fraction of visible radiation emitted from the bulb was enough to generate the fluorescence in the fibers. All the measurements were normalized by detecting the fluctuations of the light source inside the furnace with other silica multimode optical fiber connected to other fiber-optic spectrometer.

Before performing the measurements, we made a calibration of the temperature inside the furnace by using the thermocouple. Fig. 2 shows the temperature variation in the furnace when, starting from 30 °C, an increase of 10 °C is applied each 20 min up to 90 °C. The red points are the temperature given by the thermocouple placed inside the furnace. It can be seen that the heat rate of the furnace is not constant in all the temperature intervals. It decreases from an approximate rate of 1.2 °C/min at the 30–40 °C interval to 0.8 °C/min at the final step, in the 80–90 °C one. In all steps, after a transient state the temperature reaches a quasi-stable state, where the temperature can be considered constant. The duration of the time intervals with quasi-constant temperature varies from around 10 min at 40 °C to 7 min at 90 °C. Short lengths of fibers (around 5 cm) were used to ensure the thermalization of the samples at a given temperature, the uniformity of the heating and the non-inclusion of other fluorescence effects, such the reabsorption processes and propagation losses. Different types of temperature dependent measurements have been performed: short-term measurements where the temperature follows the step profile shown in Fig. 2 during 120 min

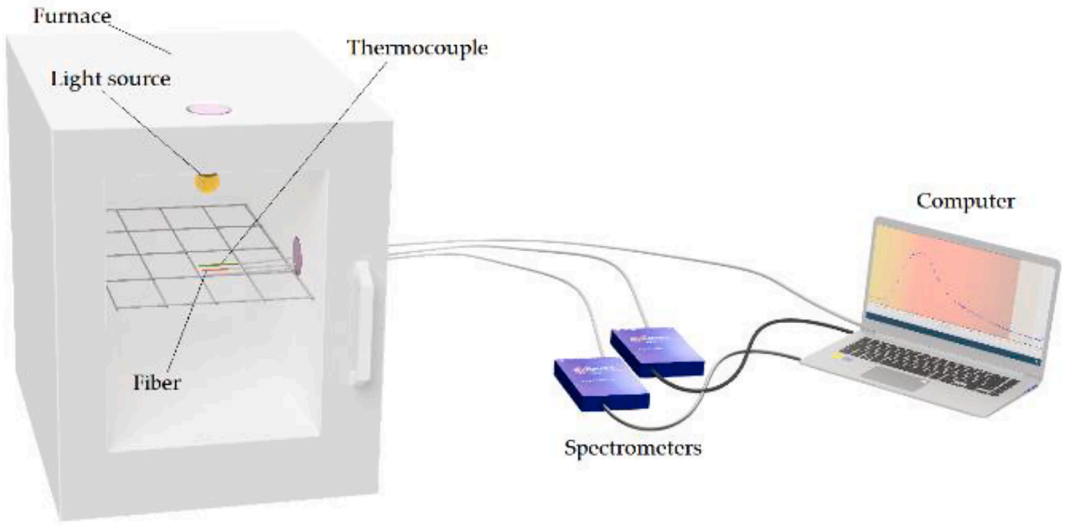

Fig. 1. Experimental set-up for the measurement of the temperature effects on the fiber sample.

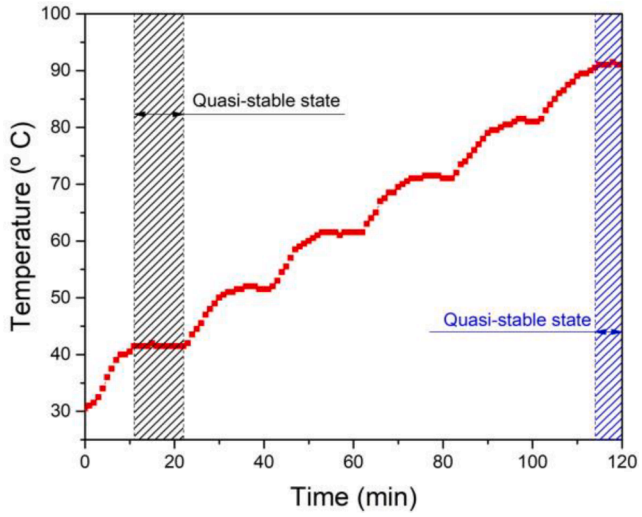

Fig. 2. Time evolution of the measured temperature in the furnace in the 30–90 °C range. Quasi-stable states of temperature in the first step (from 30 °C to 40 °C) and in the last one (from 80 °C to 90 °C).

and thermal cycles of 420 min between 30 °C and 90 °C. We have also performed long-term measurements, keeping the temperature constant during 2 days (at 30 °C and 90 °C).

The fibers analyzed in this study are POFs doped with the commercially available perylene derivative dyes, LR and LO. The fibers were fabricated by the authors using the casting method for the preform manufacturing [24]. The Lumogen series of dyes developed by BASF combine high quantum efficiency together with low photodegradation and they were specifically designed for LSCs. The host polymer is Poly (methyl-methacrylate) (PMMA) in all cases. The highest temperature used (90 °C) is just below the glass transition temperature of PMMA. No deformation of the analyzed fiber samples was detected after heating/cooling them. The characterization of the fibers as solar concentrators has been also carried out in [24].

Table 1 summarizes the main characteristics of the two fibers analyzed. Photographs of both doped fibers, excited by the sunlight, are shown in Fig. 3. The fiber sample analyzed in each experiment had not been previously used.

3. Results and discussion

In the first measurements we have analyzed the fluorescence spectra emitted by the doped fibers as the temperature is increased from 30 °C up to 90 °C in steps of 10 °C with a total time of illumination of 2 h (see Fig. 2). The fluorescence spectra of the two fiber samples obtained at three temperatures are shown in Fig. 4. The final spectrum at a given temperature has been calculated by averaging the obtained spectra over the quasi-stable state, that is, over the interval where the temperature is almost constant (see Fig. 2). The fluorescence spectra correspond to the radiative transition $S_1 \rightarrow S_0$ of the dyes embedded in the POFs. From Fig. 4, we observe that the broad emission bands of these Lumogen dyes are shifted to longer wavelengths as the temperature increases and that the intensity of the bands at 90 °C has decreased in comparison with that at 30 °C. This effect can be seen in Fig. 5 where the normalized fluorescence intensity of each fiber sample as a function of temperature has been displayed. It can be observed that the output intensity of both fibers decreases almost linearly along the measurement range, with a total reduction of around 20–25 %. The most likely mechanisms that contribute to the decrease in fluorescence intensities as temperature increases in both dyes are the nonradiative processes associated to vibrational relaxations of the molecules and of the surrounding matrix (PMMA). Although LR molecule has a higher volume and molecular weight [25], the obtained results indicate that the vibrational relaxations are not strongly influenced by the molecular structural pattern of the organic dyes. Another mechanism responsible of the decreasing of the intensity with temperature could be the guide mode leakage arising from the decrease of the refractive index of the fiber core (PMMA) as the temperature is increased (the thermo-optic coefficient of PMMA is around -1.0×10^{-4} /K) [26]. The reason for that lies in the fact that the output intensity from the end of the fiber is proportional to the number of guided modes propagating through the fiber and these are proportional to the square of the refractive index of the fiber core [27].

We have analyzed the dependence of the characteristics of the emitted spectra on temperature by calculating their average wavelengths and root-mean-square (rms) spectral bandwidths. Fig. 6 shows the dependence of the average wavelengths of the emission spectra on temperature. As can be seen, there is a red shift of the average wavelengths as the temperature is increased, which can be considered to be linear at first sight. This temperature-related shift may have a range of origins, all of them associated to changes that occur both, in the dyes and in the host matrix (PMMA polymer). These include, among others, thermally activated changes in the dye orientation in the host matrix as the temperature is increased or the variation of the PMMA refractive index with temperature causing shifts in the fluorescence peak. By fitting a linear function to the experimental points plotted in Fig. 6, we have estimated the effect of changing the temperature on the emission wavelength for our fiber samples. The slopes of the two curves obtained from the fittings, which provide the temperature sensitivities, are displayed in Table 2. Regarding the rms spectral bandwidths, they hardly vary with temperature. The obtained values have been included in Table 2. Emission wavelengths against temperature have also been described by linear fittings in quantum dots embedded in PMMA [28]. The origins of these shifts were related to the temperature dependence of the bandgap of the quantum dots and to the thermo-optic effect of the PMMA [29].

In order to analyze the behavior of LSCs under more real operating conditions, we have applied thermal cycles to the fiber that shows better performance as LSC, namely the LR-doped fiber [24]. The simulated thermal cycles are shown in Fig. 7. The sample was heated up to 90 °C and it was maintained at that temperature during 20 min. Afterwards, it was cooled down to 30 °C and it was maintained at that temperature during other 20 min. This heating and cooling cycle was repeated successively four times. Fig. 7(a) shows the time variation of the intensity during the heating and cooling cycles. It can be observed that when the sample is heated up to 90 °C in the first cycle the intensity decreases around 25 %, in agreement with the results obtained in the previous experiment (see Fig. 5). When the temperature is lowered again to 30 °C the original intensity is not totally recovered, a 10 % is lost. However, the variation of the intensity during the next heating and cooling cycles remains quite stable and at the end only a small decrease (3–4 %) of the intensity at 30 °C and at 90 °C is observed. This trend suggests that, after

Table 1
Properties of the analyzed fiber samples. The index of refraction of the fibers is uniform.

Fiber code	Type	Dopant	Conc. wt %	Diameter (mm)	Excited fiber length (cm)	Non-excited fiber length (cm)	Specific heat (PMMA) (J/kg·K)
LR-c3	Uncladded	Lumogen F Red 305	0.03	0.98 ± 0.05	5.5 ± 0.1	3.4 ± 0.05	1466
LO-c3	Uncladded	Lumogen F Orange 240	0.03	0.93 ± 0.01	5.5 ± 0.1	3.4 ± 0.05	1466

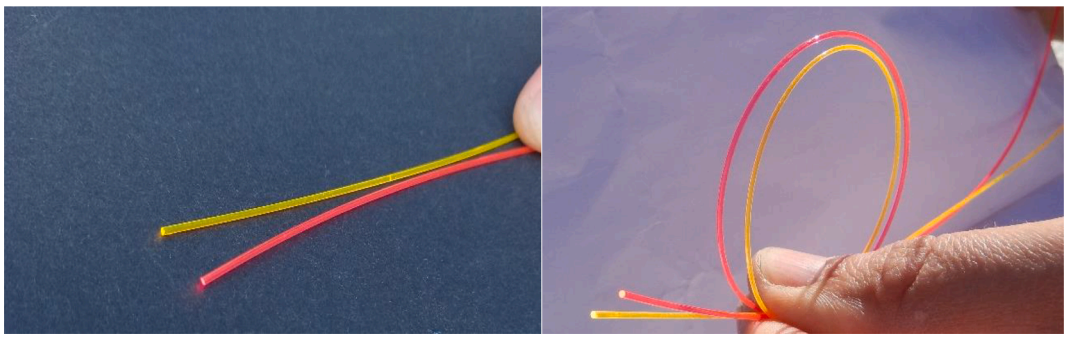

Fig. 3. Outdoor photographs of the emission of two doped fibers being excited by sunlight.

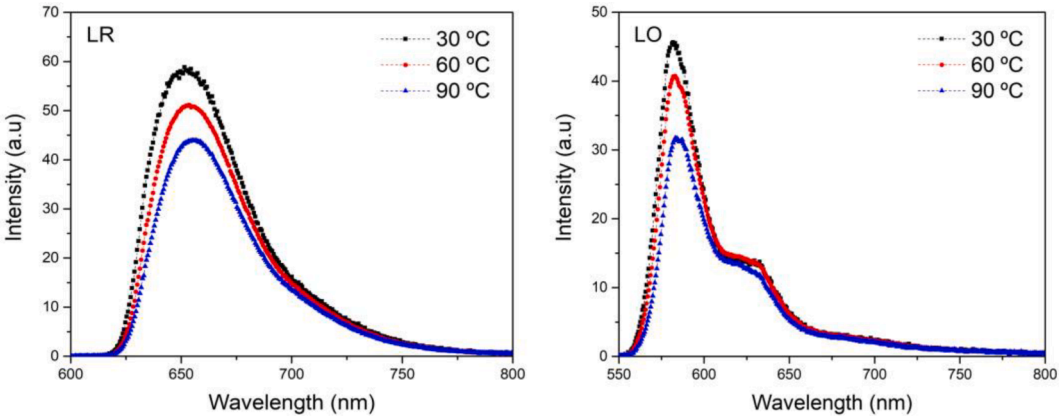

Fig. 4. Fluorescence spectra emitted from 5.5 cm long fiber samples at three different temperatures.

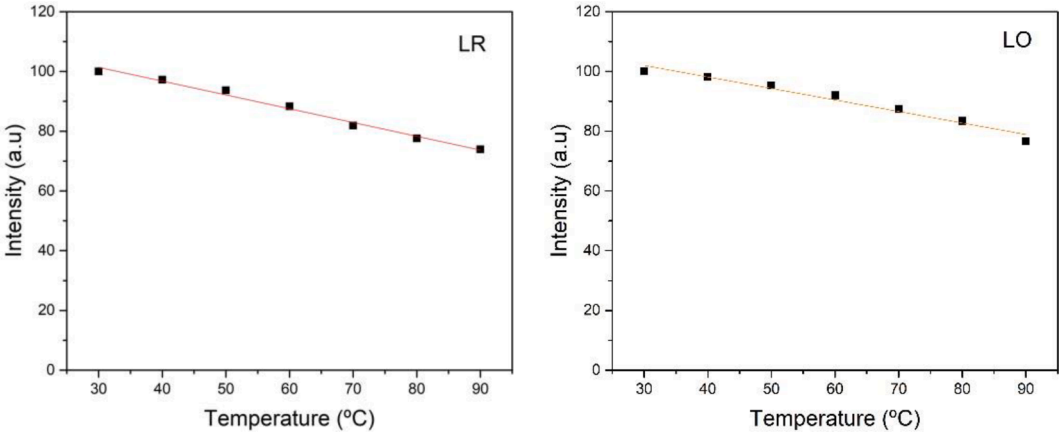

Fig. 5. Output intensity of the fiber samples as a function of temperature. The illuminated fiber length is 5.5 cm in both cases. The solid lines are the linear fittings to the data points. The relative errors of data are around 2 %.

the first cycle, when the sample is kept-up to 30 °C during 20 min, an almost full recovery of the thermal degradation occurs. In similar experiments carried out with samples composed of PMMA doped with Rhodamine B and Rhodamine 6G dyes a partial recovery of the thermal degradation was detected when the samples were heated up to 74 °C and slowly cooled to room temperature. That recovery decreased during the successive cycles [19].

The thermal cycles lead also to shifts of the emission spectra (see Fig. 7(b)). When the sample is heated up to 90 °C in the first cycle, the average wavelength shows a red-shift similar to that obtained in Fig. 6. When the sample is cooled down to 30 °C, the emission spectra is blue-shifted. The red/blue shifts are repeated during the subsequent heating/cooling cycles, respectively. If the evolution of the average emission wavelength is analyzed in more detail, we observe that when the sample is cooled down after the first heating and heated again, the average wavelengths of the emission at 30 °C and 90 °C do not return to their initial positions; they are slightly blue-shifted. The blue-shift is stronger during the first cycle (approximately 1.3 nm at 30 °C and 0.4 nm at 90 °C) and smaller during the next cycles of cooling and heating (see Fig. 7(b)).

With the aim of determine the origin of the intensity loss and the blue shifts of the emission during the heating/cooling cycles, we have analyzed the time evolution over two days of the emitted fluorescence spectra of the same doped fiber at the minimum and at the maximum

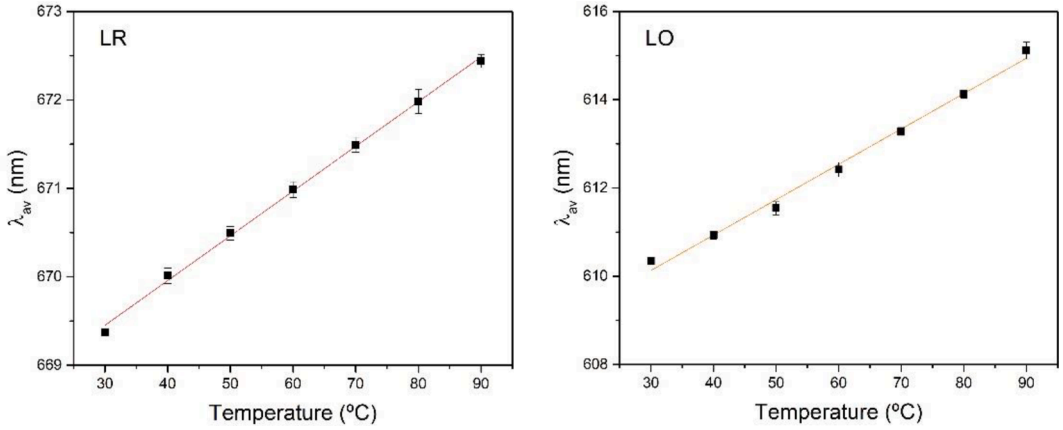

Fig. 6. Average wavelength of the emission bands as a function of temperature. The illuminated fiber length is 5.5 cm in both cases. The solid lines are the linear fittings with slopes being 0.051 nm/°C and 0.08 nm/°C for LR and LO, respectively.

Table 2
Temperature sensitivity obtained from the linear fittings of the experimental points of Fig. 6. R^2 is the coefficient of determination of the linear fitting.

Sample	$d\lambda_{av}/dT$ (nm/°C)	R^2	rms spectral bandwidth (nm)
LR-c3	0.051 ± 0.001	0.99	32 ± 1
LO-c3	0.080 ± 0.003	0.99	39 ± 3

temperature of the cycles (i.e., at 30 °C and at 90 °C, respectively). The time dependence of the intensity and of the average wavelength of the emission spectra for a LR sample at both temperatures is shown in Fig. 8. We have plotted in Fig. 8(a) the time evolution of the intensities at constant temperature normalized with the initial value of the intensity at 30 °C. We can notice that the initial intensity value at 90 °C is around 20 % lower than that obtained at 30 °C, in agreement with the previous results shown in Figs. 5 and 7(a). As we have shown, one part of this

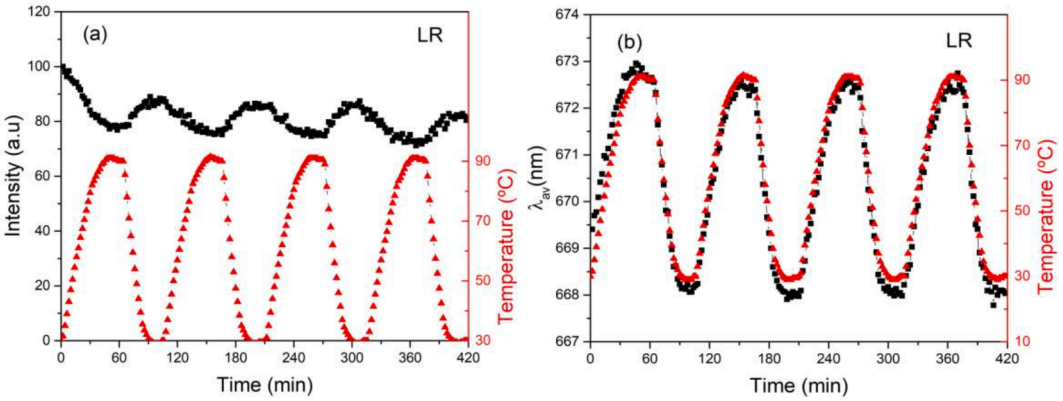

Fig. 7. (a) Time evolution of temperature and emission intensity in a LR fiber sample under the action of cyclic heating and cooling. (b) Time evolution of temperature and average emission wavelength of the LR sample under the action of cyclic heating and cooling. The illuminated fiber length is 5.5 cm.

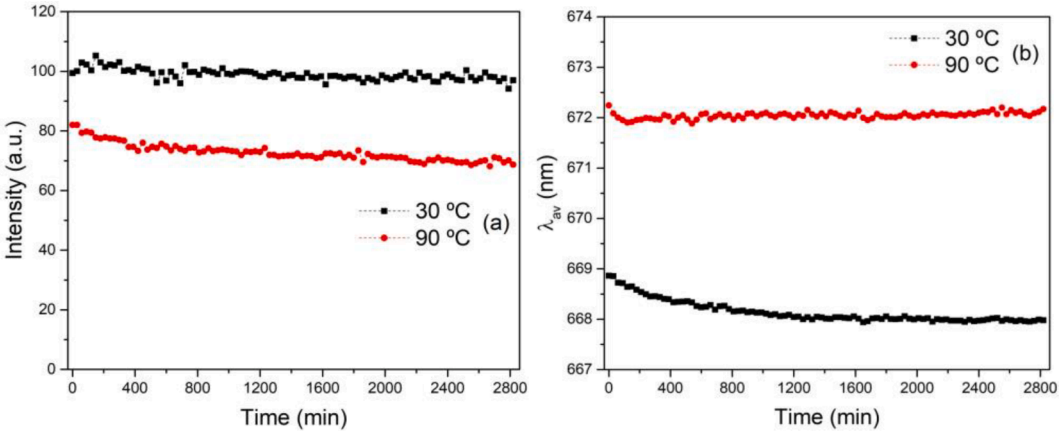

Fig. 8. Time evolution of emission intensity (a) and of average wavelength (b) at two temperatures for the LR fiber. The illuminated fiber length is 5.5 cm in both temperatures.

previous temperature dependent damage is irreversible (approx. a 10 %). In addition, from Fig. 8(a) it can be deduced that a thermally non-activated damage is also taking place since the intensity at both constant temperatures slowly decreases approximately at the same rate. These irreversible losses could be due to a decrease of the fraction of fluorescent dyes, which is related to the blue shift of the emission wavelengths. It is a well-known fact that the optical bands shift to lower wavelengths as the dye dopant concentration decreases. Indeed, we have detected this effect in POFs doped with different LR concentrations [24]. Fig. 8(b) shows the time evolution of the emission average wavelengths at 30 °C and 90 °C. As can be seen, the blue-shifts at both temperatures are similar to those observed in the cycles of Fig. 7(b). Contrary to the effects associated to reversible thermally activated processes, the effects related to the decrease of the fraction of fluorescent dyes, i.e. an intensity loss together with a blue shift of the emission spectra, show no signs of being reversible.

Finally, we have plotted in Fig. 9 the emission spectral shifts of the cycles shown in Fig. 7(b) as a function of temperature. The figure exhibits more clearly, how the temperature evolution of the emission wavelengths converges to a stable situation after the first cycle. The temperature sensitivity of the fiber sample increases slightly from 0.059 ± 0.001 nm/°C in the first heating to 0.071 ± 0.002 nm/°C in the stable situation. These values for the LR fiber sample are slightly different from those displayed in Table 2 indicating that the temperature sensitivity, in addition to its dependence on dye and on polymer matrix, it also depends on the heating/cooling rate. Similar effects to those observed in our LR doped fiber have been detected in systems based on quantum dots embedded in PMMA [28,29]. In particular, a decrease of the intensity, together with a red–shift of fluorescence bands when temperature increases and an increase of the intensity together with a blue-shift of the fluorescence spectra when temperature decreases was observed [28]. In [29], upon three cycles of heating and cooling, a stationary situation with a constant relation between emission wavelength and temperature was reached, as happens to our LR-doped fiber after the first cycle. The temperature sensitivity values obtained in these systems [29] are similar to those obtained in our study.

4. Conclusions

In this work, we have presented an experimental study on the heating up to 90 °C of two polymer optical fibers doped with dye derivatives from perylene, with the same concentration: Lumogen red and Lumogen orange. We have shown that when the fibers are heated, over 2 h, from 30 °C to 90 °C, the emission bands of the two fibers are linearly red-shifted and that the emitted intensity by both fibers decreases almost linearly with temperature. The total intensity loss in both samples is around 20–25 %. By subjecting the Lumogen red fiber to heating/cooling cycles, with temperature oscillations from 30 °C to 90 °C, about half of the intensity lost in the first cycle is recovered when the sample is cooled down to 30 °C in the following cycles. This decrease/increase of the fluorescence intensity during cycling could be explained by reversible thermal activation/deactivation processes associated to vibrations of the dye molecules and polymer matrix, and to leakage/increase of the guided modes in the fiber. In addition to the intensity recovery, we have observed linear red and blue shifts in the emission spectra as the temperature changes. These could be due to thermally activated changes in the dye orientation in the host matrix or to the variations of the polymer matrix's refractive index with temperature. Along with these reversible effects, an intensity loss together with a blue shift of the emission spectra have also been observed. By measuring the emission spectra of a sample of the same doped fiber over two days at 30 °C and at 90 °C, we have shown that the origin of those effects could be related to a small decrease of the fraction of fluorescent molecule dyes.

The finding of an almost full self-recovery in our doped polymer optical fiber, when it is subjected to temperature cycles up to 90 °C, ensures the applicability of these fiber-based luminescent solar concentrators in very high temperature environments on the Earth surface, or even expand their applicability to Space Solar Power Systems. Moreover, the temperature sensitivities provided by our doped polymer optical fibers (around 0.07 nm/°C) could even add some new functions to them, such as the sensitivity to their surrounding temperature. In other words, these fiber-based luminescent solar concentrators could also serve as indicator to visualize and monitor dynamic processes due to external stimuli, as temperature changes. All these results open new doors for the application of these luminescent materials under different and realistic external conditions of solar radiation.

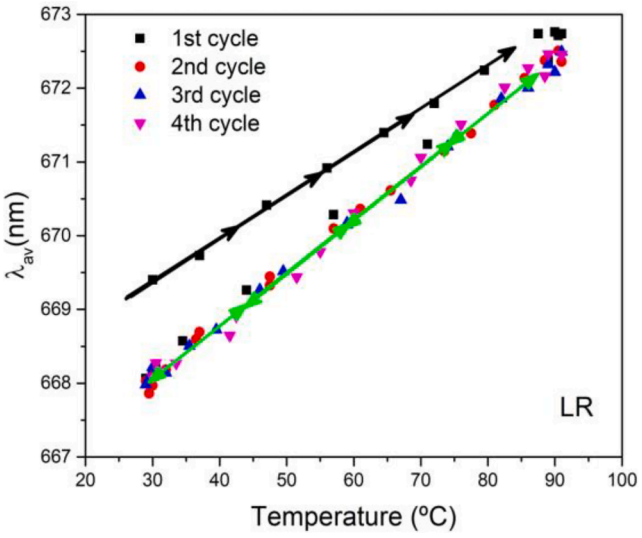

Fig. 9. Average wavelengths of the emission spectra of a LR sample as a function of temperature under the action of cyclic heating and cooling. Black line represents the linear fit in the first heating. Green line represents the stable situation reached after the first cycle. The illuminated fiber length is 5.5 cm. (For interpretation of the references to colour in this figure legend, the reader is referred to the web version of this article.)

CRediT authorship contribution statement

Jon Grandes: Resources, Investigation, Methodology, Validation, Visualization. **María Asunción Illarramendi:** Conceptualization, Methodology, Validation, Writing – original draft, Funding acquisition. **Eneko Arrospide:** Resources, Investigation, Validation, Visualization. **Iñaki Bikandi:** Validation, Visualization. **Ibon Aramburu:** Validation, Formal analysis, Writing – original draft. **Nekane Guarrotxena:** Resources, Writing – original draft. **Olga García:** Resources. **Joseba Zubia:** Funding acquisition.

Declaration of Competing Interest

The authors declare that they have no known competing financial interests or personal relationships that could have appeared to influence the work reported in this paper.

Acknowledgments

Ministerio de Ciencia, Innovación y Universidades (MAT2014-57429-R, PGC2018-095364-B-I00, PID2021-122505OB-C31, TED2021-129959B-C21); Gobierno Vasco/Eusko Jaurlaritza (IT1452-22); ELKARTEK (KK-2021/00082, KK-2021/00092)

References

[1] Y. Koike, Fundamentals of Plastic Optical Fibers, 1st ed., Wiley-VCH Verlag GmbH & Co. KGaA, Weinheim, Germany, 2015.

[2] J. Arrue, F. Jiménez, I. Ayesta, M.A. Illarramendi, J. Zubia, Polymer-Optical-Fiber Lasers and Amplifiers Doped with Organic Dyes, Polym. (Basel) 3 (2011) 1162–1180, https://doi.org/10.3390/polym3031162.
[3] W.H. Weber, J. Lambe, Luminescent greenhouse collector for solar radiation, Appl. Opt. 15 (1976) 2299, https://doi.org/10.1364/AO.15.002299.
[4] K.R. McIntosh, N. Yamada, B.S. Richards, Theoretical comparison of cylindrical and square-planar luminescent solar concentrators, Appl. Phys. B Lasers Opt. 88 (2007) 285–290, https://doi.org/10.1007/s00340-007-2705-8.
[5] T. Wang, B. Yu, B. Chen, Z. Hu, Y. Luo, G. Zou, Q. Zhang, A theoretical model of a cylindrical luminescent solar concentrator with a dye-doping coating, J. Opt. 15 (2013), https://doi.org/10.1088/2040-8978/15/5/055709.
[6] S.F.H. Correia, P.P. Lima, P.S. André, M.R.S. Ferreira, L.A.D. Carlos, High-efficiency luminescent solar concentrators for flexible waveguiding photovoltaics, Sol. Energy Mater. Sol. Cells. 138 (2015) 51–57, https://doi.org/10.1016/J.SOLMAT.2015.02.032.
[7] R.H. Inman, G.V. Shcherbatyuk, D. Medvedko, A. Gopinathan, S. Ghosh, Cylindrical luminescent solar concentrators with near-infrared quantum dots, Opt. Express 19 (2011) 24308, https://doi.org/10.1364/OE.19.024308.
[8] I. Parola, D. Zaremba, R. Evert, J. Kielhorn, F. Jakobs, M.A. Illarramendi, J. Zubia, W. Kowalsky, H.-H. Johannes, High performance fluorescent fiber solar concentrators employing double-doped polymer optical fibers, Sol. Energy Mater. Sol. Cells 178 (2018) 20–28, https://doi.org/10.1016/J.SOLMAT.2018.01.013.
[9] K. Jakubowski, C.-S. Huang, A. Gooneie, L.F. Boesel, M. Heuberger, R. Hufenus, Luminescent solar concentrators based on melt-spun polymer optical fibers, Mater. Des. 189 (2020) 108518, https://doi.org/10.1016/j.matdes.2020.108518.
[10] Y. Li, X. Zhang, Y. Zhang, R. Dong, C.K. Luscombe, Review on the Role of Polymers in Luminescent Solar Concentrators, J. Polym. Sci. Part A Polym. Chem. 57 (2019) 201–215, https://doi.org/10.1002/pola.29192.
[11] J. Roncali, Luminescent Solar Collectors: Quo Vadis? Adv. Energy Mater. 10 (2020) https://doi.org/10.1002/aenm.202001907.
[12] I. Papakonstantinou, M. Portnoi, M.G. Debije, The Hidden Potential of Luminescent Solar Concentrators, Adv. Energy Mater. 11 (2020) 2002883, https://doi.org/10.1002/aenm.202002883.
[13] M.H. Sanders, R.J. Sedwick, Thermal Design and Performance of a Luminescent Solar Concentrator for Space Power Generation, J. Spacecr. Rockets 56 (2019) 1831–1837, https://doi.org/10.2514/1.A34361.
[14] D. Du, J. Darkwa, G. Kokogiannakis, Thermal management systems for Photovoltaics (PV) installations: A critical review, Sol. Energy 97 (2013) 238–254, https://doi.org/10.1016/j.solener.2013.08.018.
[15] V.A. Rajkumar, C. Weijers, M.G. Debije, Distribution of absorbed heat in luminescent solar concentrator lightguides and effect on temperatures of mounted photovoltaic cells, Renew. Energy 80 (2015) 308–315, https://doi.org/10.1016/j.renene.2015.02.003.
[16] G. Griffini, L. Brambilla, M. Levi, M. Del Zoppo, S. Turri, Photo-degradation of a perylene-based organic luminescent solar concentrator: Molecular aspects and device implications, Sol. Energy Mater. Sol. Cells 111 (2013) 41–48.
[17] G.D. Peng, Z. Xiong, P.L. Chu, Fluorescence Decay and Recovery in Organic Dye-Doped Polymer Optical Fibers, J. Light. Technol. 16 (1998) 2365. http://www.osapublishing.org/jlt/abstract.cfm?URI=jlt-16-12-2365.
[18] B.R. Anderson, M.G. Kuzyk, Imaging studies of photodegradation and self-healing in anthraquinone derivative dye-doped PMMA, Phys. Chem. Chem. Phys. 22 (2020) 28154–28164, https://doi.org/10.1039/D0CP05426G.
[19] F.J. Meseguer, F. Cussó, F. Jaque, C. Sánchez, Temperature effects on the efficiency of Luminescent Solar Concentrator (LSC) for photovoltaic systems, J. Lumin. 24–25 (1981) 865–868, https://doi.org/10.1016/0022-2313(81)90106-X.
[20] B. Liu, S. Ren, G. Han, H. Zhao, X. Huang, B. Sun, Y. Zhang, Thermal effect on the efficiency and stability of luminescent solar concentrators based on colloidal quantum dots, J. Mater. Chem. C 9 (2021) 5723–5731, https://doi.org/10.1039/D0TC05466F.
[21] I.A. Carbone, K.R. Frawley, M.K. McCann, Flexible, Front-Facing Luminescent Solar Concentrators Fabricated from Lumogen F Red 305 and Polydimethylsiloxane, Int. J. Photoenergy 2019 (2019) 8680931, https://doi.org/10.1155/2019/8680931.
[22] F.J. Ostos, G. Iasilli, M. Carlotti, A. Pucci, High-Performance Luminescent Solar Concentrators Based on Poly(Cyclohexylmethacrylate) (PCHMA) Films, Polym. (Basel) 12 (2020), https://doi.org/10.3390/polym12122898.
[23] D.M. de Clercq, S.V. Chan, J. Hardy, M.B. Price, N.J.L.K. Davis, Reducing reabsorption in luminescent solar concentrators with a self-assembling polymer matrix, J. Lumin. 236 (2021) 118095, https://doi.org/10.1016/j.jlumin.2021.118095.
[24] E. Arrospide, M.A. Illarramendi, I. Ayesta, N. Guarrotxena, O. García, J. Zubia, G. Durana, Effects of Fabrication Methods on the Performance of Luminescent Solar Concentrators Based on Doped Polymer Optical Fibers, Polym. (Basel) 13 (2021), https://doi.org/10.3390/polym13030424.
[25] I. Parola, M.A. Illarramendi, F. Jakobs, J. Kielhorn, D. Zaremba, H.-H. Johannes, J. Zubia, Characterization of Double-Doped Polymer Optical Fibers as Luminescent Solar Concentrators, Polym. (Basel) 11 (2019) 1187, https://doi.org/10.3390/polym11071187.
[26] Z. Zhang, P. Zhao, P. Lin, F. Sun, Thermo-optic coefficients of polymers for optical waveguide applications, Polym. (Guildf) 47 (2006) 4893–4896, https://doi.org/10.1016/j.polymer.2006.05.035.
[27] Allan W. Snyder, John D. Love, Optical Waveguide Theory, Springer, Boston, MA, n.d. 10.1007/978-1-4613-2813-1_29.
[28] Y. Chen, W. Luan, S. Zhang, F. Yang, Quantum-dots based materials for temperature sensing: effect of cyclic heating-cooling on fluorescence, J. Nanoparticle Res. 21 (2019) 185, https://doi.org/10.1007/s11051-019-4629-8.
[29] H.C.Y. Yu, S.G. Leon-Saval, A. Argyros, G.W. Barton, Temperature effects on emission of quantum dots embedded in polymethylmethacrylate, Appl. Opt. 49 (2010) 2749–2752, https://doi.org/10.1364/AO.49.002749.